PHOTOBLINKING/PHOTOBLEACHING DIFFERENTIAL EQUATION MODEL FOR INTENSITY DECAY OF FLUORESCENCE MICROSCOPY IMAGES

[1,2]*Isabel Rodrigues and* [1,3]*João Sanches*

[1]Institute for Systems and Robotics
[2]Instituto Superior de Engenharia de Lisboa
[3]Instituto Superior Técnico
Lisbon, Portugal

ABSTRACT

Fluorescence confocal microscopy images are affected by fading effects, such as *photblinking* and *photobleaching*, that leads to image intensity decreasing along the time, preventing long exposure time experiments. These fading effects increase with the amount of radiation that illuminates the speciem. Additionally, these type of images present a low *signal to noise ratio* and are corrupted by a type of multiplicative noise with Poisson distribution due to the strong amplification needed to observe the small fluorescent radiation emitted by the fluorosphore. Therefore a trade-off exists between the needs of increasing the incident radiation to improve the *signal to noise ratio* and the needs of decreasing that radiation to minimize the fading effects.

The main goal of this paper is to obtain an intensity decay law to describe the *photoblinking/photobleaching* effect based on a theoretical model derived from the quantic phenomena described in the literature, involved in the process. The decay law, derived here from the theoretical model, matches the intensity decay law that is usually referred in the literature, obtained from experimental data. The model is plugged in a Bayesian denoising algorithm that takes into account the temporal correlation among consecutive images to improve its visualization, mainly in the last ones where the intensity is very small.

Results with real data is presented to illustrate the validity of the model.

***Index Terms*—** Photobleaching, photoblinking, differential model, denoising, Poisson

1. INTRODUCTION

Fluorescence confocal microscopy (FCM) is a powerful biological image modality [1] used to observe *in-vivo* dynamic process occurring inside the cells. In this technique, tagging proteins, *e.g. Green Fluorescent Protein* (GFP), fluoresce when radiated with a specific wavelength laser making it possible to track single or groups of molecules involved in very specific biochemical processes to be studied.

The radiation emitted by the fluorescent proteins is very weak and must be highly amplified. By this, the corresponding images are usually corrupted by a type of multiplicative noise with Poisson distribution and simultaneously its overall intensity decays along time.

Correspondent author: Isabel Rodrigues (irodrigues@isr.ist.utl.pt). This work was supported by Fundação para a Ciência e a Tecnologia (ISR/IST plurianual funding) through the POS Conhecimento Program which includes FEDER funds.

This fading effect consists on a reversible, *photoblinking*, or permanent, *photobleaching*, ability loss of the fluorophore to fluoresce along the time that prevents long time experiments. The corresponding decay rate depends mainly on the amount of energy radiated over the specimen. Therefore a trade-off exists between the needs of increasing the incident radiation to improve the *signal to noise ratio* of the image and the needs of decreasing that radiation to minimize the fading effects.

An accurate model for this intensity decay is important in the definition of the right observation model in order to obtain effective denoising algorithms for this type of images. In this work a continuous *second order differential equation* (2DE) dynamic model describing the *photoblinking/photobleaching* (PBB) effect is proposed in section 2. The 2DE model is built by taking into account the known quantic phenomena involved in the process that are described in the literature.

The main novelty of this paper is the intensity decay law describing the PBB effect, derived from the proposed 2DE model, that matches the one that is usually used in the literature, obtained from experimental data [2, 3].

The proposed intensity decay law is included in a denoising algorithm, designed in a Bayesian framework with the *maximum a posteriori* (MAP) criterion, where the temporal correlation of consecutive images in the sequence is taken into account. With this approach it is possible to strongly attenuate the noise and enhance the images, even in the last ones within the sequence where the information is highly corrupted by noise and hidden due the PBB effect.

Tests with real data are presented to illustrate the validity of the model and a denoising example with real FCM images is also shown.

The paper is organized as follows. Section 2 derives the dynamic model that describes the *photoblinking/photobleaching* effect based on the quantum effects involved and in information obtained from the literature. Section 3 describes the Bayesian denoising algorithm where the *photoblinking/photobleaching* effect is taken into account. Section 4 present experimental results with real data and section 5 concludes the paper.

2. MODEL

From a fluorescence point of view, fluorescent tagging molecules can be in three main states (see Fig.1), i) *ON-state*, where they are able to fluoresce and be observed, ii) *OFF-state*, where they are not able to fluoresce and therefore are not visible and finally at the iii) *BLEACHED-state* where they become permanently *OFF*. The molecules stay at each *OFF-state* and *ON-state*, called *active* states, according to a power distribution [4] and they can commute between

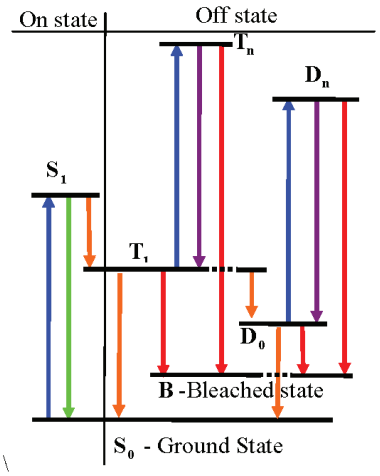

Fig. 1. Photoblinking and photobleaching electronic state transition diagram. S denotes excited *singlet states* and T and D denotes the excited *triplet* and *anion* states respectively. Blue arrows denote transitions for higher energy levels, Green ones stay for transitions for lower levels with fluorescence emission of radiation, orange and magenta transitions for non *BLEACCHED* states and red ones denotes permanently transitions for *BLEACHED-states*.

these two states, but are not able to recover from the *BLEACHED-state* state. The mean intensity of an image at a given time instant is assumed to be proportional to the number of fluorescent molecules in the *ON-state*. In this section, a continuous time *differential equation* dynamic model is proposed to describe the number of molecules in the *ON-state* and *OFF-states* along the time.

Let n be the total number of active fluorescent molecules where n_{ON} of them are in the *ON* state and the remaining n_{OFF} are in the *OFF* state. The time intervals at each state are governed by *Levy statistics* [4] following a power distribution [5], $p(\tau_r) = c_r \tau_r^{-a_r}$, where $r \in \{ON, OFF\}$. The power law distribution associated with these time intervals is related with the so called effect of *statistical aging* that leads to a constant increasing on the time intervals at each state along the time [4]. Additionally, it was experimentally confirmed that $a_{ON} > a_{OFF}$ [5] which means that the fluorescent molecules spend more time in the *OFF-state* than in the *ON-state*, or equivalently, the relative number of transitions from the *ON-state* to the *OFF-state* is larger than the relative number of reverse transitions. Therefore, since the molecules spend more and more time in the *OFF-state* [5], the probability of transitions decreases with time and is always higher from the *ON-state* to the *OFF-state* than the reverse. This non stationary reversible process of transitions between the *ON* and *OFF* states leads to a constant image fading along the time called *photoblinking*.

The *photobleaching*, on the contrary, is a non-reversible process where the fluorescent molecules loose its ability to fluoresce. As noted in [6] the transitions to the permanent dark states occur only from the excited states. Here, however, the model proposed in [7] is adopted, where the *photobleaching* from the *ON-state* is discarded. In this model, displayed in Fig.1, it is assumed that no *photobleaching* occurs form the excited singlet state, S_1 but only from the *OFF-states*, composed by the triplet, T_{1-n}, and anion, D_{1-n}, states. The transitions to the permanent dark state are represented in Fig.1 by the red arrows.

The Jablonski diagram displayed in Fig.1 suggests the following set of differential equations to describe the dynamics of the *photo-blinking/photobleaching* effect

$$n(t) = n_{ON}(t) + n_{OFF}(t) \quad (1)$$

$$\frac{dn_{ON}}{dt}(t) = \beta_{OFF} n_{OFF}(t) - \beta_{ON} n_{ON}(t) \quad (2)$$

$$\frac{dn}{dt}(t) = -\xi n_{OFF}(t) \quad (3)$$

where $n(t)$ is the total number of active molecules at instant t and $n_{ON}(t)$ and $n_{OFF}(t)$ are the number of active molecules in the *ON-state* and *OFF-state* respectively, at the same time. $\xi = I + \tau$ is the decay rate of the active molecules associated with the transitions to the permanent *BLEACHED-state* where I is proportional to the amount of incident radiation and τ is associated with other factors not related with illumination. This means that even when no radiation illuminates the specimen, $I = 0$, the number of active molecules decreases. However, since the main factor for intensity decay is the incident radiation it is expected that $I >> \tau$.

Equation (2) models the *photoblinking* effect where it is assumed that the variation of the number of molecules in the *ON-state* is proportional, with constant β_{OFF}, to the number of molecules at the *OFF-state* and negatively proportional, with constant β_{ON}, to the number of molecules in the *ON-state*. The magnitudes of β_{ON} and β_{OFF} are related with the previously referred *statistical aging* effect [4] that leads to an increasing number of active molecules in the *OFF-state* and a correspondent decreasing number in the *ON-state*. Therefore, the transition rate from the *OFF-state* to the *ON-state* is smaller than the inverse transition, which means that $\beta_{ON} > \beta_{OFF}$

The equation (3) models the *photobleaching* effect where it is assumed that the total variation on the number of active molecules is proportional, with constants τ and I, to the number of molecules in the *OFF-state*, because only transitions from the *OFF-state* to the *BLEACHED-state* are admissible in the model used in this paper (see red arrows in Fig.1).

According to [6], the main cause of the *photobleaching* is the "illumination history". However in [7] the authors refer other important factors to the *photobleaching*, such as the moist and the temperature. The overall effect of theses factors is modeled in equation (3) by the constant $\tau < I$.

From the set of equations (1-3) the following second order differential equation describes the dynamics of the number of molecules in the *ON-state*, that is directly related with the intensity of the image,

$$\frac{d^2 n_{ON}(t)}{dt^2} + (\alpha + \xi)\frac{dn_{ON}(t)}{dt} + \beta_{ON}\xi n_{ON}(t) = 0 \quad (4)$$

where $\alpha = \beta_{ON} + \beta_{OFF}$. The Laplace transform of $n_{ON}(t)$ when the initial conditions are $n_{ON}(0) = n^0_{ON}$ and $\frac{dn_{ON}}{dt}(0) = \dot{n}^0_{ON}$, is

$$N_{ON}(s) = \frac{as + b}{(s + \lambda_1)(s + \lambda_2)} \quad (5)$$

where $a = n^0_{ON}$, $b = (\alpha + \xi) n^0_{ON} + \dot{n}^0_{ON}$ and

$$\lambda_{1,2} = \frac{\alpha + \xi}{2} \mp \frac{\sqrt{\Delta(\xi)}}{2} \quad (6)$$

with the discriminant

$$\Delta(\xi) = \xi^2 - 2\underbrace{(\beta_{ON} - \beta_{OFF})}_{>0}\xi + \alpha^2 \quad (7)$$

The roots of (7), $\xi_{1,2} = \beta_{ON} - \beta_{OFF} \pm 2\sqrt{-\beta_{ON}\beta_{OFF}}$, are always complex because $\beta_{ON}, \beta_{OFF} > 0$. Therefore the discriminant (7)

is always positive, $\Delta(\xi) > 0$, which means that the poles $\lambda_{1,2}$ are always real.

The inverse Laplace transform of (5) is

$$n_{ON}(t) = \gamma e^{-\lambda_1 t} + (a-\gamma)e^{-\lambda_2 t}, \qquad t \geq 0 \tag{8}$$

where

$$\gamma = \frac{a\lambda_1 - b}{\lambda_1 - \lambda_2} \tag{9}$$

The intensity decay law described by (8) and derived from (1-3), matches the experimentally based model referred in the literature where the *photoblinking/photobleaching* effect is expressed in terms of two decaying exponentials.

3. SEQUENCE DENOISING

In this section the denoising algorithm for Poisson FCM images with the *Photoblinking/Photobleaching* model included, is described. The denoising algorithm described here is an improvement of the algorithm described in [8] where the *photoblinking/photobleaching* model described here was incorporated in the data observation model.

Each data sequence of FCM images is denoted by a 3D tensor, $\mathbf{Y} = \{y_{i,j,t}\}$, with $0 \leq i,j,t \leq N-1, M-1, L-1$. Each data point, $y_{i,j,t}$, is corrupted with Poisson noise and the time intensity decrease due to the *photobleaching* effect is modeled by a weighted sum of two decaying exponentials with constant rates, λ_1 and λ_2 as derived in section 2. Each pixel of the noiseless sequence, $\mathbf{X}$, can then be written as $x_{i,j,t} = f_{i,j,t}\eta(t)$ where

$$\eta(t) = e^{-\lambda_1 t} + \gamma e^{-\lambda_2 t} \tag{10}$$

and $\mathbf{F} = \{f_{i,j,t}\}$, with $0 \leq i,j,t \leq N-1, M-1, L-1$ stands for the underlying morphology of the cell nucleus. γ, λ_1 and λ_2 are constants estimated in the fitting process of the model to the mean image intensities along the sequence $\overline{y}(t) = \Gamma\eta(t,\Theta) + r(t)$ where $r(t)$ are the residues, Γ is a constant that is discarded and $\Theta = \{\hat{\lambda_1}, \hat{\lambda_2}, \hat{\gamma}\}$.

The ultimate goal of the proposed algorithms is to estimate the cell nucleus underlying morphology, $\mathbf{F}$, from the noisy data, $\mathbf{Y}$, exhibiting a low *signal to noise ratio* (SNR). A Bayesian approach using the *maximum a posteriori* (MAP) criterion is adopted to estimate $\mathbf{F}$. This problem may be formulated as the following energy optimization task

$$(\hat{\mathbf{F}}) = \arg\min_{\mathbf{F}} E(\mathbf{F}, \mathbf{\Theta}, \mathbf{Y}) \tag{11}$$

where the energy function $E(\mathbf{F}, \mathbf{\Theta}, \mathbf{Y}) = E_Y(\mathbf{F}, \mathbf{\Theta}, \mathbf{Y}) + E_F(\mathbf{F})$ is a sum of two terms, $E_Y(\mathbf{F}, \mathbf{\Theta}, \mathbf{Y}) = -\log(p(\mathbf{Y}, \mathbf{F}, \Theta))$ called the *data fidelity term* and $E_F(\mathbf{F}) = -\log(p(\mathbf{F}))$ called the *prior* term for $\mathbf{F}$. The first term pushes the solution toward the observations according to the type of noise corrupting the images and the *a prior* energy term penalizes the solution according with some previous knowledge about $\mathbf{F}$, in this case a stepwise function [9]. Assuming the independence of the observations, the *data fidelity term*, which is the negative of the log-likelihood function, is defined as

$$E_Y(\mathbf{F}, \mathbf{\Theta}, \mathbf{Y}) = -\log\left[\prod_{i,j,t=0}^{N-1,M-1,L-1} p(y_{i,j,t}|f_{i,j,t}, \mathbf{\Theta})\right], \tag{12}$$

where $p(y_{i,j,t}|f_{i,j,t}, \mathbf{\Theta}) = \frac{\left(f_{i,j,t}\hat{\eta}(t)\right)^{y_{i,j,t}}}{y_{i,j,t}!} e^{-\left(f_{i,j,t}\hat{\eta}(t)\right)}$ is the Poisson distribution and $\hat{\eta}(t)$ is given by (10).

By assuming $\mathbf{F}$ as a *Markov Random Field* (MRF), $p(\mathbf{F})$ can be written as a Gibbs distribution, $p(\mathbf{F}) = \frac{1}{T}\exp[-\sum_{c\in C} V_c(\mathbf{F})]$, where T is the normalizing constant and $V_c(.)$ are the *clique potentials* [10]. The negative of the argument of the exponential functions in $p(\mathbf{f})$ is called *energy* and will be denoted by $E_F(\mathbf{F})$. In this paper log-Euclidean [11] based potential functions are used since they produce edge-preserving priors which are the most convenient to keep the cell nucleus morphology and simultaneously to remove the noise in the homogeneous regions. Therefore the overall problem consists on the minimization of the following function

$$\begin{aligned} E(\mathbf{F}, \mathbf{\Theta}, \mathbf{Y}) &= \sum_{i,j,t}[f_{i,j,t}\hat{\eta}(t) - y_{i,j,t}(\log(f_{i,j,t}) + \log\hat{\eta}(t))] \\ &+ \alpha\sum_{i,j,t}\sqrt{\log^2\left(\frac{f_{i,j,t}}{f_{i-1,j,t}}\right) + \log^2\left(\frac{f_{i,j,t}}{f_{i,j-1,t}}\right)} \\ &+ \beta\sum_{i,j,t}\sqrt{\log^2\left(\frac{f_{i,j,t}}{f_{i,j,t-1}}\right)}. \end{aligned} \tag{13}$$

where α and β are tunning parameters to reduce or increase the strength of the regularization in the space and time dimensions respectively.

4. EXPERIMENTAL RESULTS

Five sequences of real FCM images of the nucleus of a HeLa cell [12], denoted by $G26$, $G100$, $FLIP_0$, $FLIP_1$ and $FLIP_2$ were tested for denoising using the proposed photobleaching model. $G26$ consists of 26 registered images of a cell nucleus, acquired with constant low intensity laser illumination, at a rate of 23s. $G100$ is a sequence of 100 images of a cell nucleus, acquired in the same experimental conditions as $G26$. $FLIP_0$, $FLIP_1$ and $FLIP_2$ sequences are the result of using the *fluorescence loss in photobleaching* (FLIP) technique during the acquisition process with the purpose of inducing intense diffusion and transport activities inside the nucleus. The sampling rate is $3.6s$ in these three sequences.

The mean *per* image was computed for all the sequences and the resulting curves were fitted with the described two-exponentials model using a non linear least squares procedure. The original curves (dotted blues line) and the fit results (continuous red lines) are shown in Figs. 2. The root mean square error (RMSE), displayed in table 1, evince the adequacy of the theoretically derived model to describe the global photobleaching effect in this imaging modality even in the presence of diffusion and transport phenomena. The denoising results for sequence $G26$ are presented in Fig. 3 and show the suitability of proposed model to cope with both the photobleaching effect and the Poisson noise on what concerns to the reconstruction of the cell morphology. Also the edge preserving abilities of the adopted prior potential functions are noticeable in this figure.

5. CONCLUSIONS

In this paper a continuous *second order differential equation* dynamic model for the *fluorescence confocal* image intensity decay is presented. This model is based on the quantic mechanisms involved in the *photobleaching* process that are summarized in a Jablonski diagram displayed in Fig.1. The solution of the model for a given set of initial conditions leads to the same intensity decay law that several authors have adopted, based only on experimental data. Denoising

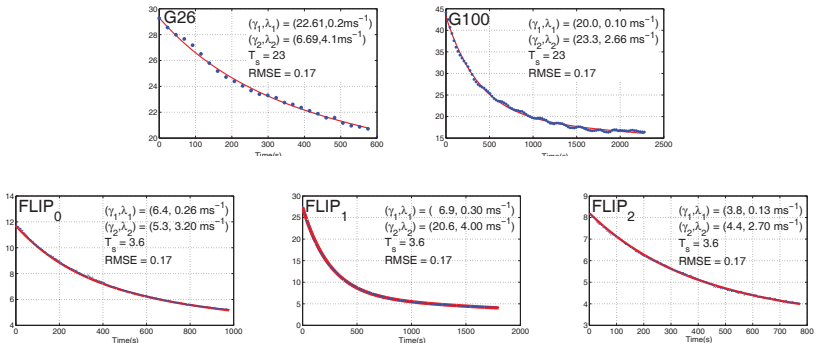

Fig. 2. Mean intensity *per* image (blue dotted line) and respective curve fittings by a two negative exponential model (red continuous line). $\gamma_1 = \gamma$ and $\gamma_2 = a - \gamma$.

Seq.	γ	$a-\gamma$	$\lambda_1 \times 10^{-4}$ s^{-1}	$\lambda_2 \times 10^{-4}$ s^{-1}	RMSE
$G26$	22.61	6.69	2.00	41.00	0.17
$G100$	19.96	23.26	0.96	26.61	0.36
$FLIP_0$	6.36	5.34	2.60	32.00	0.043
$FLIP_1$	6.85	20.56	2.95	40.00	0.086
$FLIP_2$	3.82	4.39	1.32	27.00	0.043

Table 1. Model parameters and *root mean square error* (RMSE) for sequences $G26$, $G100$, $FLIP_0$, $FLIP_1$ and $FLIP_2$. Model: $\overline{y}(t) = \gamma e^{-\lambda_1 t} + (a-\gamma)e^{-\lambda_2 t}$.

results using the proposed model show its adequacy to describe the global *photoblinking/photobleaching* effects.

6. ACKNOWLEDGMENT

The authors thank Dr. José Rino and Prof^a Maria do Carmo Fonseca, from the Instituto de Medicina Molecular de Lisboa, for providing biological technical support.

7. REFERENCES

[1] Jeff W. Lichtman and José-Angel Conchello, "Fluorescence microscopy," *Nature Methods*, vol. 2, pp. 910–919, November 2005.

[2] Nathalie B. Vicente, Javier E. Diaz Zamboni, Javier F. Adur, Enrique V. Paravani, and Victor H. Casco, "Photobleaching correction in fluorescence microscopy images," *Journal of Physics: Conference Series*, vol. 90, pp. 012068 (8pp), 2007.

[3] S. Gavrilyuk, S. Polyutov, P. C. Jha, Z. Rinkevicius, H. Ågren, and F. Gel'mukhanov, "Many-photon dynamics of photobleaching," *J. Phys. Chem.*, vol. 111, no. 47, pp. 11961–11975, 2007.

[4] X. Brokmann, J.-P. Hermier, G. Messin, P. Desbiolles, J.-P. Bouchaud, and M. Dahan, "Statistical aging and nonergodicity in the fluorescence of single nanocrystals," *Physical review letters*, vol. 90, no. 12, 2003.

[5] Jörg Schuster, Jörg Brabandt, and Christian von Borczyskowski, "Discrimination of photoblinking and photobleaching on the single molecule level," *Journal of Luminescence*, vol. 127, no. 1, pp. 224–229, November 2007.

[6] P. Didier, L. Guidoni, and F. Bardou, "Infinite average lifetime of an unstable bright state in the green fluorescent protein," *Phys. Rev. Lett.*, vol. 95, no. 9, pp. 090602, Aug 2005.

[7] R. Zondervan, F. Kulzer, M. A. Kol'chenko, and M. Orrit, "Photobleaching of Rhodamine 6G in Poly(vinyl alcohol) at the ensemble and single-molecule levels," *J. Phys. Chem. A*, vol. 108, no. 10, pp. 1657–1665, March 2004.

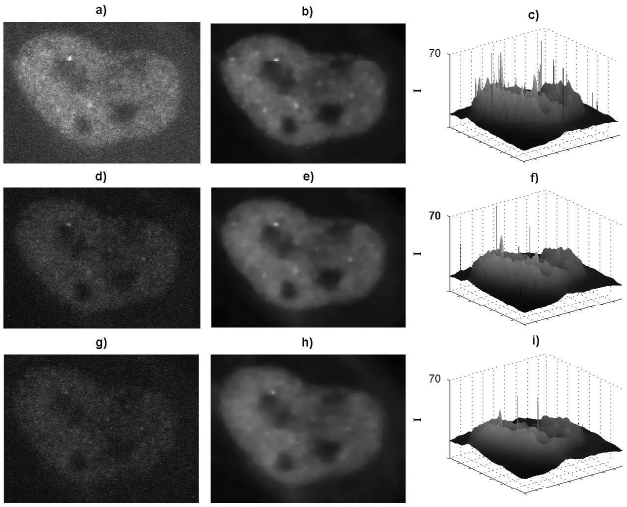

Fig. 3. Sequence $G26$: Images 1, 10 and 17 from the sequence of 26 images. a), d), g) noisy original data; b), e), h) estimated cell nucleus morphology; c), f), i) mesh representations of the respective estimated morphologies.

[8] Isabel Rodrigues, Joao Xavier, and Joao Sanches, "Fluorescence confocal microscopy imaging denoising with photobleaching," in *Engineering in Medicine and Biology Society, 2008. EMBS 2008. 30th Annual International Conference of the IEEE*, Aug. 2008, pp. 2205–2208.

[9] Todd K. Moon and Wynn C. Stirling, *Mathematical methods and algorithms for signal processing*, Prentice-Hall, 2000.

[10] S. Geman and D. Geman, "Stochastic relaxation, Gibbs distributions, and the bayesian restoration of images," *IEEE Transactions on Pattern Analysis and Machine Intelligence*, vol. PAMI, no. 6, pp. 721–741, Nov. 1984.

[11] Vincent Arsigny, Pierre Fillard, Xavier Pennec, and Nicholas Ayache, "Log-Euclidean metrics for fast and simple calculus on diffusion tensors," *Magnetic Resonance in Medicine*, vol. 56, no. 2, pp. 411–421, August 2006.

[12] D.A. Jackson, F.J. Iborra, E.M. Manders, and P.R. Cook, "Numbers and organization of RNA polymerases, nascent transcripts, and transcription units in HeLa nuclei," *Mol Biol Cell*, vol. 9, pp. 1523–1536, 1998.